Investigation of the Liquid Crystalline−Isotropic Phase Transition in Oligo(phenylenevinylene) with Alkyl Side Chains

William Zhu, Wenjie Li, and Luping Yu*

Department of Chemistry and The James Frank Institute, The University of Chicago, 5735 South Ellis Avenue, Chicago, Illinois 60637

Received May 9, 1997; Revised Manuscript Received August 2, 1997[⊗]

ABSTRACT: Variable-temperature ^{13}C NMR T_1 and NOE measurements were performed on alkyl-substituted oligo(phenylenevinylene) (OPV) melts at two Larmor frequencies. The existence of a liquid crystalline (LC) phase in OPV was demonstrated by DSC and polarized microscopy experiments. The NMR data showed that while the OPV backbone behaves like a liquid crystal, the side chains act merely as a "solvent". The backbone ^{13}C T_1 data were fitted to a modified log χ^2 distribution, and information regarding backbone rotational dynamics was extracted from the fitting. It was found that the backbone rotational dynamics slow down as the OPV sample crosses from the LC phase into the isotropic phase. Instead of a sharp transition, the OPV LC−isotropic phase transition occurs in a temperature window of 2−3 °C. The composition of the two phases in the biphasic region was also calculated from the T_1 data as a function of temperature.

Introduction

We report here variable-temperature ^{13}C NMR T_1 (spin lattice relaxation time) and NOE (nuclear Overhauser enhancement) studies on oligo(phenylenevinylene) with alkyl side chains (OPV), below and above the liquid crystalline (LC)−isotropic phase transition. Our group has described the syntheses of well-defined oligo(phenylenevinylene)s with alkoxy side groups.[1] These OPVs were synthesized in order to couple with other functional polymers to form diblock copolymers. It was also demonstrated that these OPV molecules are liquid crystals within a certain temperature range. More recently, we utilized these molecules to prepare light-emitting diodes (LEDs) which exhibit sizable quantum yields.[2] The combination of the liquid crystallinity and LED raised very interesting questions. For example, can we align these molecules in a magnetic field? What will happen to the LED performance if these molecules can be aligned in a magnetic field? Before we could answer these questions, the dynamic behavior of OPV in a magnetic field had to be studied. Unlike conventional small molecule liquid crystals, the OPV molecule consists of a rigid backbone and flexible side chains (so-called 'hairy rod' molecules). Theoretical studies by Ballauff[3] on 'hairy rod' molecules indicated that the side chains play the role of a 'bound solvent'. We hoped to provide experimental evidence to support Ballauff's claims. Answering these questions is the motivation behind this study. Our experimental results seem to support the 'bound solvent' idea; the T_1 data for side chain carbons showed no sudden changes in the LC−isotropic phase transition. Furthermore, the activation energies of C−H bond orientation in the side chains are higher than those in *n*-octane. This indicates that the 'solvent' is indeed 'bound'. The dynamics of the rigid backbone slow down significantly in the liquid crystal to isotropic (LC−isotropic) phase transition region, indicating that the rigid backbone rotates along the long molecular axis when they are in the LC phase. In the following section, a detailed experimental procedure and theoretical fitting are presented.

[⊗] Abstract published in *Advance ACS Abstracts,* September 15, 1997.

Experimental Section

Sample Preparation. A six-aromatic-ring oligo(phenylenevinylene) with an iodo end group was first synthesized according to ref 4. Then the iodo end group was reduced with lithium aluminum hydride. For NMR measurements, the sample was degassed prior to being sealed under vacuum.

DSC Measurements and Polarized Microscopy. The differential scanning calorimetry measurements were performed on a DSC-10 system from TA Instruments. The heating rate was 5 °C/min. For comparison with the pristine OPV, a sample was annealed at 150 °C for 1 h before the DSC measurement. The annealing of the OPV sample and the DSC measurements were all performed under a nitrogen atmosphere.

The polarized microscopic observations were carried out on a Nikon (HFX-IIA) microscope equipped with a Linkman (TMS-90) hot stage. The clearing temperature was recorded on an annealed OPV sample at a heating rate of 10 °C/min.

NMR T_1 and NOE Measurements. Spin−lattice relaxation times (T_1) and nuclear Overhauser enhancements (NOE) were measured under conditions of complete proton decoupling. ^{13}C T_1 data were collected on GE Omega-500 and GE Omega-300 spectrometers at Larmor frequencies of 125.8 and 75.6 MHz, respectively. A $\pi-t-\pi/2$ pulse sequence was used in the T_1 measurements with a delay of at least 8 times T_1 after each acquisition. NOE values were measured at 125.8 MHz by a comparison of spectra with continuous decoupling and inverse-gated decoupling, waiting at least 10 times T_1 between acquisitions. All the NMR experiments were done without sample spinning in order to avoid the possibility of magnetohydrodynamic interference. The reproducibility of T_1 is within 5%, and that of NOE is within ±0.1.

The temperature range of the NMR measurements was from the OPV melting point to the high-temperature specification of the NMR probes. The temperature stability was within ±0.5 °C. T_1 data were found to be a weak function of time at the same temperature, especially in the LC phase. In order to perform NMR measurements on a well-aged sample, the sample was annealed at the experimental temperature for 1 h before each NMR measurement. However, the T_1 results may still not represent the equilibrium values.

Data Analysis

Relaxation Equations. In OPV melts, the dominant relaxation mechanism of ^{13}C nuclei is the dipole−dipole interaction with their bonded protons except for the methyl carbon and the quaternary carbon. We are mostly interested in the NMR data of the methylene and the methine carbon.

S0024-9297(97)00653-0 CCC: $14.00

In this case, T_1 is related to the reorientation of the C−H bond by the following equation:[5]

$$\frac{1}{T_1} = Kn[J(\omega_H - \omega_C) + 3J(\omega_C) + 6J(\omega_C + \omega_H)] \quad (1)$$

Here, n is the number of bonded protons and K is a constant related to the C−H bond length. K is 2.42×10^9 s^{-2} for the methine carbon and 2.29×10^9 s^{-2} for the methylene carbon.[6] ω_H and ω_C are the Larmor frequencies of proton and carbon. The spectral density function $J(\omega)$ is the Fourier transform of the correlation function CF(t):

$$J(\omega) = \int_0^\infty \mathrm{CF}(t)\, e^{i\omega t}\, dt \quad (2)$$

where CF(t) is defined as

$$\mathrm{CF}(t) = \frac{1}{2}\langle 3(\mathbf{e}_x(t)\cdot\mathbf{e}_x(0))^2 - 1\rangle \quad (3)$$

In eq 3, $\mathbf{e}_x(t)$ is a unit vector in the direction of the C−H bond at time t. The brackets indicate an ensemble average.

The shape of CF(t) is determined by the mechanism of the C−H vector orientation. The rate of C−H bond reorientation may be characterized by a model-independent, rotational correlation time τ_c:

$$\tau_c = \int_0^\infty \mathrm{CF}(t)\, dt \quad (4)$$

The relationship between T_1 and τ_c is simplified in the extreme narrowing regime, where the frequency of the C−H vector orientation is much faster than the Larmor frequency. In this case, τ_c is inversely proportional to T_1:

$$\frac{1}{T_1} = 10nK\tau_c \quad (5)$$

Three criteria exist as the indications of the extreme narrowing regime. The first is that NOE equals three, the second is that T_1 is independent of Larmor frequency, and the third is that T_1 equals T_2. In this work, NOE data were collected and backbone T_1 data were measured at two Larmor frequencies. Therefore we defined the extreme narrowing region by the first two criteria only.

Fitting Procedure. In this paper, T_1 data are fitted by a modified log χ^2 distribution.[7] The modified log χ^2 distribution consists of two parts. A single exponential with a relaxation time τ_0 represents the minor part of the correlation function that corresponds to motions much faster than the NMR Larmor frequencies. The amplitude of the single exponential is defined by a constant A. Since NMR T_1 is not sensitive to the temperature dependence of these motions, τ_0 is fixed at 1 ps and A is chosen to be temperature independent. The major and slower part of the correlation function is represented by a log χ^2 distribution with a characteristic time $\bar{\tau}$ and width parameter p. In our fitting p is temperature independent and $\bar{\tau}$ has an Arrhenius temperature dependence. More details regarding the fitting procedure may be found in refs 7 and 8.

Results and Discussion

DSC and Polarized Microscopy Measurements. Shown in Figure 1 are the DSC traces of both pristine and annealed OPVs. While the pristine oligomer has virtually one peak, the annealed oligomer shows two sharp endothermic transitions at 115 and 127 °C. This result indicates that OPV forms a liquid crystalline phase and that these two transitions correspond to its melting and its clearing temperatures. Polarized microscopy pictures taken on OPV melts (see Figure 2) revealed the typical Schlieren texture for a nematic liquid crystalline phase. The clearing point was determined to be around 127 °C.

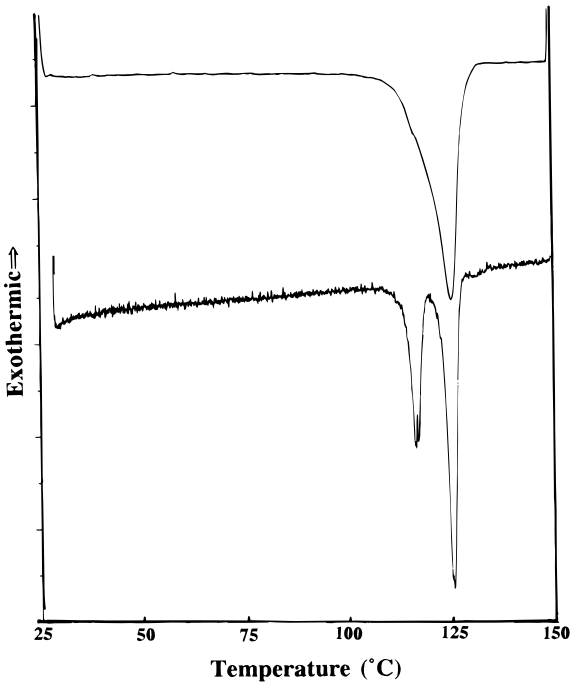

Figure 1. DSC traces of OPV. The top is the heating curve of pristine polymer. The bottom is the heating curve of an annealed sample.

Figure 2. Polarized microscopy of OPV at 122 °C.

Figure 3 shows the peak assignments of the OPV ^{13}C NMR spectrum in melts. These assignments have been made by DEPT (distorsionless enhancement by polarization transfer) experiments and comparison to spectra of alkanes and similar OPVs.[9] NMR T_1 measurements were performed on peaks j, i, h, g, c, and def. The relaxations of carbon k and a nuclei have significant contributions from mechanisms other than dipolar interactions, such as chemical shift anisotropy and spin rotation. Carbon b has T_1 values that require long term experiments. Thus, no T_1 or NOE data were collected on carbons a, b, or k. The peaks for carbons d, e, and f overlap. Therefore, the data on peaks d, e, and f represent the average of these three types of carbons.

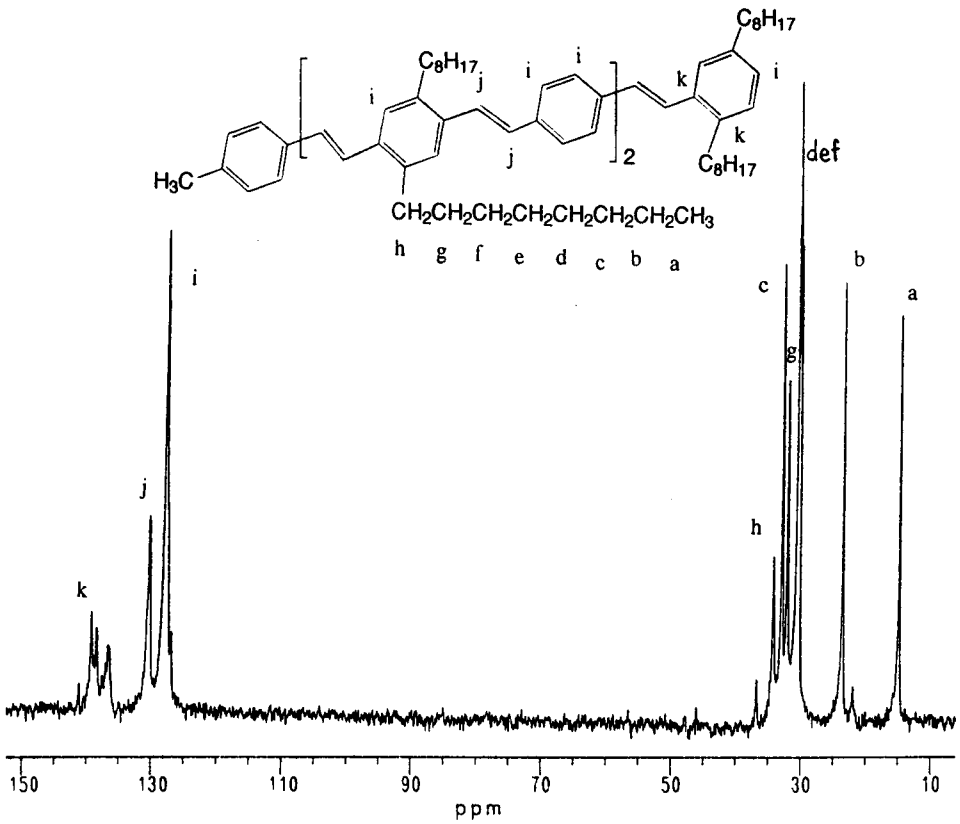

Figure 3. ^{13}C spectrum of OPV melts at 125.8 MHz. The temperature is 140 °C.

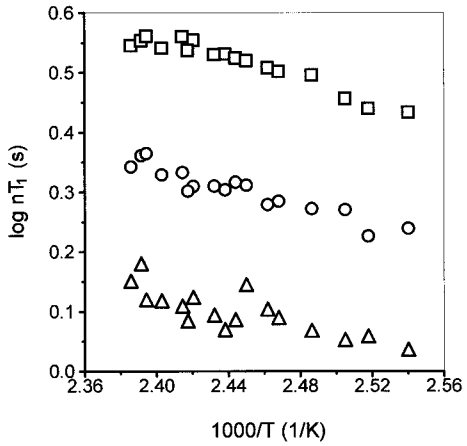

Figure 4. ^{13}C T_1 data of the side chains at 125.8 MHz vs temperature. Different symbols represent different carbons: (□) carbon c; (○) carbons d, e, and f; (△) carbon g. *n* cooresponds to the number of protons attached to the carbon, and in this figure, $n = 2$.

The data on peak **i** are the average of all aromatic methine carbons.

C−H Vector Orientation of the Side Group Carbons. We first turn our attention to the motions of side groups and their dependence on temperature in the LC−isotropic transition. Shown in Figure 4 is the nT_1 for various carbons in the side chains. When the reorientations of C−H vectors are sufficiently fast, the T_1 value increases with increasing temperature. This is the case in Figure 4. Thus qualitatively, a longer T_1 corresponds to faster dynamics in Figure 4. The T_1 values for carbon h are shorter than those for carbon g at the same temperature, although the former are too noisy to be analyzed quantitatively and therefore are not shown in the figure. The general trend is that carbons closer to the backbone show shorter T_1, which indicates slower dynamics. This is not surprising given the fact that the rigid backbone hinders the motions of the side chains.

Another interesting feature of Figure 4 is that there is no sudden change of T_1 data for carbons c, d, e, and f in the LC−isotropic transition. This seems to indicate the side chains do not undergo a phase transition within the detectable range of the NMR measurements. Poly(phenylenevinylene) (PPV) with alkoxy side groups has been synthesized in this group.[9] Experimental evidence shows that longer side chains in PPV help to lower the melting and clearing temperatures. Ballauff has extended the lattice theory of Flory to rodlike systems with flexible side chains.[3] The side chains were found to act as a "bound" solvent in these systems; Figure 4 clearly supports this viewpoint.

Quantitative analysis of T_1 values for carbons d, e, f, and c may be carried out using eq 5. Figure 5 shows the NOE values of carbons d, e, f, c, and g. Within experimental error, the NOE values for carbons d, e, f, and c approach three. Therefore, all the T_1 data for carbons d, e, f, and c shown in Figure 4 are in the extreme narrowing regime. The correlation time τ_c is thus calculated from the T_1 data model-independently, and the results are shown in Figure 6. Assuming that τ_c has an Arrhenius temperature dependence, we extracted activation energies of 14 and 16 kJ/mol for the C−H bond orientation of carbons d, e, f, and c, respectively. These values are higher than those for the C−H bond orientation in *n*-octane,[10] indicating that the side chains experience steric hindrance due to the existence of the rigid rod. This implies that the 'solvent' is indeed 'bound'.

C−H Bond Orientation of the Backbone Carbons. Figures 7 and 8 show the T_1 results of two types of backbone carbons. We noticed that twists of T_1 data exist at 133 °C for two kinds of backbone carbons at both

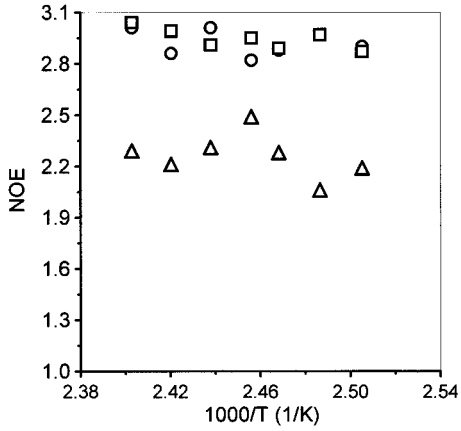

Figure 5. NOE data of the side chain carbons at 125.8 MHz vs temperature. Carbon symbols are the same as those in Figure 4.

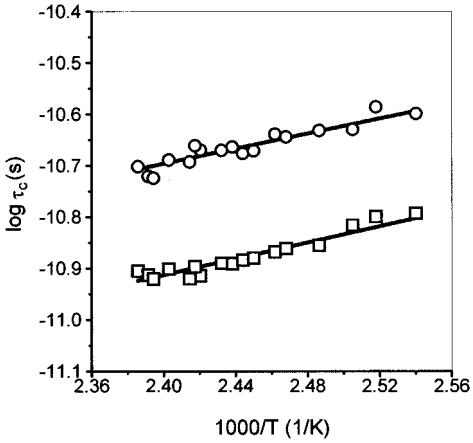

Figure 6. Temperature dependence of τ_c, the time integral of the correlation function, for the side chain carbons. Carbon symbols are the same as those in Figure 4. The solid lines are linear least square fits, which give activation energies of 14 and 16 kJ/mol for carbons def and c, respectively.

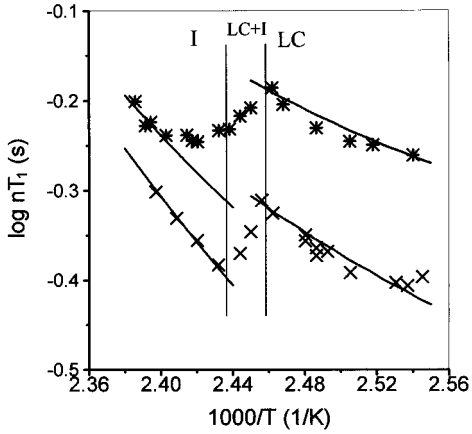

Figure 7. T_1 data of carbon j vs temperature at 125.8 MHz (*) and 75.6 MHz (×). The solid lines are fits by the modified log χ^2 distribution.

125.8 and 75.6 MHz,[11] which corresponds to the LC−isotropic phase transition. This feature is distinctively different from that of the side group carbons, whose C−H vector reorientation is undisturbed by the LC−isotropic phase transition. Within a single phase, backbone T_1 data decrease monotonically with temperature. A comparison with the side group T_1 data reveals that, at the same temperature, backbone carbons have shorter T_1 values than side group carbons. This indicates that the backbone motions are slower than the side group motions.

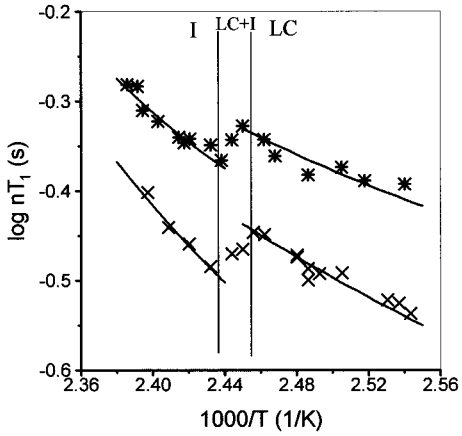

Figure 8. T_1 data of carbon i vs temperature at 125.8 MHz (*) and 75.6 MHz (×). The solid lines are fits by the modified log χ^2 distribution.

Figures 7 and 8 also show that the results are frequency dependent. The T_1 values are out of the extreme narrowing region. Thus, we cannot extract dynamics information using eq 5. However, information regarding backbone dynamics may be obtained by fitting the T_1 data to a certain model.[12] There is at present no consensus about which model best describes the experimental results. Our goal here is not to test the applicability of different models. Efforts are focused on extracting dynamic information from T_1 data in the LC−isotropic transition. For this purpose, those models capturing the essential features of C−H vector orientation are adequate. Therefore, we chose the modified log χ^2 distribution.[7] Other models, such as the DLM distribution,[13] can also be expected to fit the T_1 data.

The modified log χ^2 distribution has been used to describe the C−H vector orientation in polymer backbones. It consists of a single exponential plus a log χ^2 distribution.[14] When it is applied to the C−H vector reorientation in the OPV backbone, the single exponential represents the fast librations within the potential energy barrier and the log χ^2 distribution represents other slower motions, including local segmental motions and reorientation of the entire molecule. The librations possess frequencies much faster than the Larmor frequency. NMR T_1 data were affected by the amplitude but not the temperature dependence of the librations. For flexible polymer chains, the backbone local segmental motions and the reorientation of the whole molecule occur on different time scales. The former are usually of the order of nanoseconds, and the latter can be as long as microseconds. Our OPV molecules have a short backbone which is also rigid. Thus in OPV, the local segmental motions and the reorientation of the whole molecule should be of comparable time scales and closely correlated to each other. The analysis of backbone T_1 data would yield information regarding the whole molecule reorientation, even though the segmental motions and the orientation of the whole molecule are both responsible for the temperature dependence of T_1 data in our study. Taking these factors into consideration, we chose the following fitting procedure. The single exponential was chosen to have a fixed relaxation time of 1 ps, which is much faster than the time scale of the inverse Larmor frequency. We allow the shape and temperature dependence of the log χ^2 distribution to vary in order to give the best fit of the T_1 data at both Larmor frequencies.

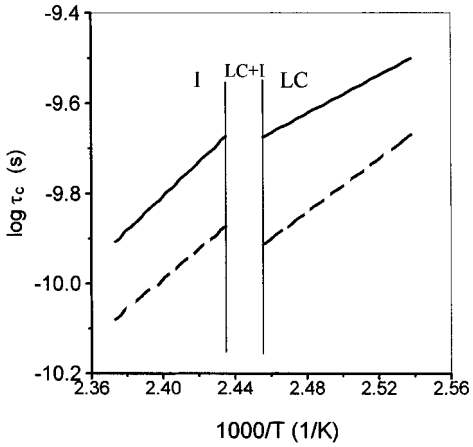

Figure 9. Time integral of the correlation function τ_c calculated from the fits in Figures 7 and 8 using eq 4. The solid lines represent carbon i, and the dashed lines represent carbon j.

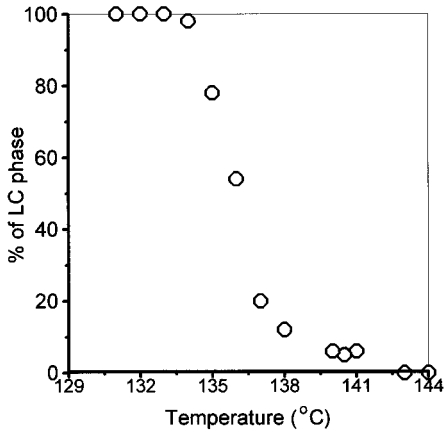

Figure 10. Composition of OPV in the LC−isotropic phase transition. The data points are calculated from the average of both carbons i and j at two Larmor frequencies.

After a correlation function is obtained from the fitting, the rotational correlation time τ_c for the backbone C−H vector orientation may be calculated using eq 4. The results are shown in Figure 9.[15] First we notice that carbon j has a smaller τ_c than carbon i, which indicates that C−H orients faster for carbon j than for carbon i. This can be explained by the fact that the double bonds are somewhat more flexible than aromatic rings. Another interesting feature is that the rotational dynamics seem to be faster in the LC region than what would be expected in this temperature range if the isotropic behavior were extrapolated, although the temperature dependence of the rotational dynamics is similar in both phases. This seems to indicate that the rigid rods rotate along the long molecular axis when they are in the LC phase. The rotational diffusion of the OPV backbone is hindered by the isotropic arrangements of the isotropic phase.

Similar phenomena in translational diffusion have been observed in other liquid crystals. For example, Murphy et al.[16] measured the translational diffusion of tetramethylsilane (TMS) in 4,4′-bis(*n*-heptyloxy)azoxybenzene (HOAB) using pulsed NMR. They observed that $D_{\parallel}$, the diffusion coefficient parallel to the HOAB long molecular axis, remained the same below and above the nematic to isotropic transition of HOAB and that $D_{\perp}$, the diffusion coefficient perpendicular to the HOAB long molecular axis, decreased by a factor of two in the nematic to isotropic phase transition. Noack[17] measured the translational self-diffusion constant D_T of *p*-azoxyanisole (PAA) by a combination of field cycling and pulsed gradient methods. He has shown that the isotropic diffusion (D_T) above the clearing point is more strongly hindered, i.e., slower than the diffusion in the ordered state parallel ($D_T^{\parallel}$) or perpendicular ($D_T^{\perp}$) to the director axis.

We noticed that, in Figures 7 and 8, the T_1 data changed continuously in the LC−isotropic phase transition. This is different from the case for small molecular liquid crystals such as PAA, whose T_1 data jump suddenly at the nematic to isotropic phase transition. We assume that in OPV there is a biphasic region where the isotropic phase and the LC phase coexist. This may be due to the fact that, compared to small molecule liquid crystals, OPV does not easily reach an equilibrium state, and thus two phases can coexist over a small temperature range. Theoretically, in the biphasic region, the T_1 inversion recovery (IR) curve should be biexponential. But experimentally a single exponential IR curve was always observed. This can be explained by the following.

A biexponential IR curve can be represented by eq 6:

$$\text{IR curve} = A_{LC}(1 - 2e^{-\tau/T_1^{LC}}) + A_I(1 - 2e^{-\tau/T_1^{I}}) \quad (6)$$

where A_{LC} and A_I are proportional to the amount of OPV in the LC and isotropic phases. T_1^{LC} and T_1^{I} are the spin lattice relaxation times in the two phases. However, when $T_1^{LC} \approx T_1^{I}$, the right side of eq 6 may be approximated as a single exponential:

$$\text{IR curve} \approx A(1 - 2e^{-\tau/T_1}) \quad (7)$$

Therefore, when two relaxation times are close to each other, a biexponential IR curve may be observed in experiments as a single exponential. In Figures 7 and 8, it is reasonable to assume that T_1^{I} and T_1^{LC} follow the extrapolation of the fittings. Thus T_1^{I} and T_1^{LC} differ from each other by no more than 30% in the biphasic region. Therefore all IR curves were single exponential in the biphasic region. This is true for the T_1 values of both carbons i and j at the two Larmor frequencies.

The parameters in eqs 6 and 7 are related to each other by the following:

$$A = A_{LC} + A_I \quad (8)$$

$$\frac{A_{LC}}{A_I} = \frac{T_1 - T_1^{I}}{T_1^{LC} - T_1} \quad (9)$$

Equation 9 can be used to calculate the composition of the biphasic region, assuming that T_1^{LC} and T_1^{I} follow extrapolation of the fittings in Figures 7 and 8. The results are presented in Figure 10. Almost 80% of OPV is converted from one phase to the other in a temperature window of 2 °C. Because the temperature was stable within ±0.5 °C in the NMR measurements, there is a relatively large error bar on the composition calculated. Nevertheless, Figure 10 demonstrates a new way to study the composition of the biphasic region in a phase transition. If the biphasic region covers a wider temperature window or the temperature stability is

better in the NMR measurements, T_1 measurements may provide a new approach in the determination of phase composition.

Conclusions

The LC−isotropic phase transition of OPV has been investigated by ^{13}C NMR, DSC, and polarized microscopy. It was found that the LC−isotropic phase transition has no effect on the T_1 data of side group carbons. On the other hand, the T_1 values of backbone carbons decrease significantly in the LC−isotropic transition. The different behaviors of the backbone and the side groups indicate that the side groups act only as a "bound solvent" in OPV melts. The backbone T_1 data were fitted to a modified log χ^2 distribution, and the time integral of the correlation function was extracted from the fitting. It was found that the rotational dynamics slow down in the LC−isotropic phase transition region. This seems to indicate that the rigid rods rotate along the longitudinal axis when they are in the LC phase and that the rotational diffusion of the OPV backbone is hindered by the isotropic arrangements of the isotropic phase. Instead of a sharp transition, the LC−isotropic phase transition in OPV occurs in a temperature window of 2−3 °C, and a biphasic region exists. The composition of the biphasic region was calculated from the NMR T_1 data. This demonstrates that NMR T_1 measurements can be used as a potential tool to study a biphasic region in a phase transition.

Acknowledgment. This work was supported by ONR and the National Science Foundation. Support from the National Science Foundation Young Investigator programs is gratefully acknowledged. This work also benefited from the support of the NSF MRSEC program at the University of Chicago.

References and Notes

(1) Maddux, T.; Li, W.; Yu, L. *J. Am. Chem. Soc.* **1997**, *119*, 844.
(2) Goodson, T.; Li, W.; Yu, L. *Adv. Mater.* **1997**, *9*, 639.
(3) Ballauff, M. *Macromolecules* **1986**, *19*, 1366.
(4) Li, W.; Morkved, T. L.; Maddux, T.; Zhu, W.; Jaeger, H. M.; Yu, L. *Polym. Prepr.*, submitted.
(5) (a) Bovey, F. A. *Nuclear Magnetic Resonance Spectroscopy*, 2nd ed.; Academic Press: San Diego, CA, 1988. (b) Abragam, A. *The Principles of Nuclear Magnetism*; Clarendon Press: Oxford, 1961.
(6) C−H bond lengths are found in: Pople, J. A.; Gordan, M. *J. Am. Chem. Soc.* **1967**, *89*, 4253.
(7) Zhu, W.; Ediger, M. D. *Macromolecules* **1995**, *28*, 7549.
(8) Zhu, W.; Ediger, M. D. *J. Polym. Sci., Polym. Phys. Ed.* **1997**, *35*, 1241.
(9) Bao, Z.; Chen, Y.; Cai, R.; Yu, L. *Macromolecules* **1993**, *26*, 5281.
(10) (a) Smith, G. D.; Yoon, D. Y. *J. Chem. Phys.* **1994**, *100*, 649. (b) Lyerla, J. R.; McIntyre, H. M.; Torchia, D. A. *Macromolecules* **1974**, *7*, 11.
(11) According to the DSC and polarized microscopy experiments, the melting and the clearing temperatures are 115 and 127 °C, respectively. The NMR measurements indicate that the LC region is between 120 and 133 °C. Although all experiments show a LC window of 12−13 °C, the temperatures in NMR measurements are shifted. This is probably due to the inaccuracy of temperature determination in the NMR spectrometers.
(12) (a) Heatley, F. *Prog. Nucl. Magn. Reson. Spectrosc.* **1979**, *13*, 47. (b) Heatley, F. *Annu. Rep. NMR Spectrosc.* **1986**, *17*, 179. (c) Dais, P.; Spyros, A. *Prog. Nucl. Magn. Reson. Spectrosc.* **1995**, *27*, 555.
(13) Dejean de la Batie, R.; Laupretre, F.; Monnerie, L. *Macromolecules* **1988**, *21*, 2045.
(14) Schaefer, J. *Macromolecules* **1973**, *6*, 882.
(15) Due to the limited temperature range of the T_1 data, good fits can be obtained by various combinations of fitting parameters. Therefore the lines in Figure 9 have larger error bars than the line width and should be used only for qualitative comparison.
(16) Murphy, J. A.; Doane, J. W.; Fishel, D. L. *Liquid Crystals and Ordered Fluids*; Johnson, J. F., Porter, R. S., Eds.; Plenum Press: New York, 1973; Vol. 2.
(17) Noack, F. *Mol. Cryst. Liq. Cryst.* **1984**, *113*, 247.

MA9706539